

Tribo-mechanical interpretation for advanced thermoplastics and the effects of wear-induced crystallization

Levente Ferenc Tóth^{1,2}, Jacob Sukumaran¹, Gábor Szabó², Patrick De Baets¹

¹ Soete Laboratory, Department of Electrical Energy, Metals, Mechanical Constructions and Systems, Ghent University, Technologiepark Zwijnaarde 46, B-9052 Zwijnaarde, Belgium. Member of Flanders Make, the strategic research center for the manufacturing industry, Belgium

² Department of Polymer Engineering, Faculty of Mechanical Engineering, Budapest University of Technology and Economics, Műegyetem rkp. 3, H-1111 Budapest, Hungary

Abstract

Despite the available knowledge in tribology of thermoplastic polymers the relation between the dominating wear mechanisms and the influencing material factors are still questionable. The present research aims to relate the tribological properties of thermoplastics to their mechanical behaviour and morphological features. Wear-induced further crystallisation of semi-crystalline polymers has been analysed in relation to measured wear and friction/bulk temperature. In this paper nine different polymers (polyamide-imide – PAI, polyether-imide – PEI, polycarbonate – PC, polyphenylsulfone – PPSU, polyethylene terephthalate – PET, ultra-high molecular weight polyethylene – UHMWPE, polyvinylidene fluoride – PVDF, polyphenylene sulfide – PPS, polyamide 6 – PA6) were compared. All specimens were tested with a large scale linear reciprocating flat-on-flat tribo-tester in dry contact condition against 100Cr6 steel counterface. A contact pressure of 4 MPa and 50 mm/s sliding speed were chosen for all the experiments. Wear testing resulted an increase in crystallinity for the semi-crystalline grades. Amongst them, PET and PPS showed a high relative increase in crystallinity. In case of these two materials, the frictional heating was sufficiently high to modify the morphology of the contact surface but still it was below the melting range. Results of instrumented indentation tests also confirm the significant crystallinity increase by showing higher hardness/spring stiffness after wear testing.

Keywords: sliding friction and wear, amorphous and semi-crystalline thermoplastics, transfer layer, wear-induced crystallinity, wear mechanism

1. Introduction

Thermoplastic polymers are often used in tribological applications because of their self-lubricating nature, internal damping capacity and their ability to operate in abrasive environment. According to their morphological structure thermoplastics are classified into amorphous and semi-crystalline materials [1, 2]. Semi-crystalline polymers also include amorphous areas that encase the crystallites as a matrix which accounts for the degree of crystallinity [3]. The degree of crystallinity can vary due to the thermal and the mechanical antecedent of the polymer and has an effect on its mechanical properties [4-6]. Because of the changes in mechanical properties and in orientation of the molecular chains, the degree of crystallinity also has a significant effect on the transfer layer formation and behaviour, which may in turn affect the friction and wear characteristics [6, 7]. Due to ongoing wear crystallinity can also vary with time. The degree of crystallinity is thus not a constant value during the whole lifecycle of a tribological component. Comparing to other plastics, semi-crystalline

thermoplastics show decreased friction and wear values due to their ability to form a uniform and adequate transfer layer during wear [8].

It is noteworthy to mention that the relationships between the degree of crystallinity/mechanical properties and the tribological characteristics of semi-crystalline thermoplastics are still not fully established. Different hypotheses have been put forward including difference in materials, environments and measurement conditions/parameters. From the researches with polyethylene terephthalate (PET) it is clear that degree of crystallinity has an effect on the friction and wear behaviour [9-11]. Bhimaraj et al. reported that the coefficient of friction decreases and the wear rate increases with increasing degree of crystallinity [9]. A possible explanation is that the increase in degree of crystallinity reduces the toughness and ductility, and hence the polymer surface loses its ability to sustain the local impacts and high strains, which then leads to higher wear rate [9], although the hardness and strength of polymers increase with increased crystallinity [12]. In case of ultra-high molecular weight polyethylene (UHMWPE) Kang et al. also introduced that higher crystallinity causes higher wear rate, comparing slowly cooled samples to quenched ones [13]. In contrast to the results with PET, Karupppiah et al. showed that both coefficient of friction and wear rate are decreasing with the increasing degree of crystallinity of UHMWPE [6]. It is noteworthy to mention that UHMWPE has much lower hardness than PET. According to them this increase in wear resistance of UHMWPE can be related to the increase in hardness and in elastic modulus [6]. The increase in hardness with the increased degree of crystallinity was also confirmed by nano-indentation tests [6]. Cartledge et al. investigated the wear resistance of polyamide 6 (PA6) as the function of the degree of crystallinity which was varied by the cooling condition of the manufacturing process [14]. It can be stated that the increase of crystallinity results an increase of the wear resistance [14]. Chen et al. state that PA66 is able to form an adequate transfer layer on steel counterfaces, while this is not true for polyphenylene sulfide (PPS) [15]. The crystalline regions in the debris are destroyed in both PA66 and PPS; therefore the degree of crystallinity in debris is significantly lower than for the original material [15].

These literature results show that the correlation between the degree of crystallinity changes and the wear rate is not fully clarified, yet, although necessary for proper design of an adequate tribo-material. Especially the link between crystallinity, mechanical properties, transfer layer formation and debris generation should be understood. Looking at real applications it is possible that, due to the wear-induced crystallisation of the contact surfaces, after an initial sliding distance the material properties change in such a way that the material performance alters in an unexpected way. In order to better understand such performance deviation it is important to determine the mechanical and tribological behaviour prior to and after the wear process.

The present paper tries to expand our knowledge in this complex topic with the application of a large scale tribo-configuration. Due to the large scale wear tests higher friction/bulk temperature is expected, which is able to affect the degree of crystallinity of the materials and in this way mechanical features as well.

2. Materials and methods

2.1. Test materials

In this research work neat amorphous and semi-crystalline thermoplastics were chosen. The materials do not include tribo-additives nor any reinforcements, as these fillers would modify the characteristics of the neat polymers causing an increased uncertainty in this research work. The specimens (Figure 1) were selected from a broad range of plastic materials with different level of performance (engineering, advanced and extreme performance). Another viewpoint for the polymer selection was the crystallinity, to compare both semi-crystalline and amorphous grades for the better understanding. All the tested materials in the present investigation were provided by Quadrant EPP Belgium.



Figure 1. Thermoplastics provided by Quadrant EPP Belgium

The investigated amorphous thermoplastics (Table 1) include Duratron® T4203 (polyamide-imide, PAI), Duratron® PEI U1000 (polyether-imide, PEI), Quadrant® PC 1000 (polycarbonate, PC) and Quadrant® PPSU (polyphenylsulfone, PPSU). The tested semi-crystalline thermoplastics (Table 2) are Ertalyte® PET-P (polyethylene terephthalate, PET), TIVAR® 1000 (ultra-high molecular weight polyethylene, UHMWPE), SYMALIT® 1000 (polyvinylidene fluoride, PVDF), Techtron® 4208 (polyphenylene sulphide, PPS) and ERTALON® 6 XAU (polyamide 6, PA6).

Table 1 and 2 introduce some important thermal and mechanical properties of the chosen thermoplastics, as extracted from Quadrant EPP datasheets. In Table 1 the glass transition temperature of amorphous materials and in Table 2 the melting temperature of semi-crystalline plastics are given. PA6 has relatively high water absorption at saturation in air (2.2% at 23°C and 50% RH), as it can be seen from Table 2. That value is 1-2 orders of magnitude higher than for the other semi-crystalline materials. In amorphous thermoplastics PAI has similarly high water absorption at saturation in air (2.5% at 23°C and 50% RH).

Table 1. Thermal and mechanical properties of amorphous thermoplastics (Quadrant EPP Belgium).

Applied materials	Duratron® T4203	Duratron® PEI U1000	Quadrant® PC 1000	Quadrant® PPSU
	polyamide- imide PAI	polyether- imide PEI	polycarbonate PC	polyphenylsulfone PPSU
Density (g/cm ³)	1.41	1.27	1.20	1.29
Water absorption at saturation in air (23°C, 50% RH, %)	2.50	0.70	0.15	0.50
Glass transition temperature (°C) DSC 20°C/min	280	215	150	220
Thermal conductivity at 23°C (W/mK)	0.26	0.24	0.21	0.30
Maximal service temperature in air (short periods, °C)	270	200	135	210
Maximal service temperature in air (20,000h, °C)	250	170	120	180
Ball indentation hardness (N/mm ²), dry material	200	165	120	95
Tensile strength (MPa)	150	129	74	83
Tensile modulus (MPa)	4200	3500	2400	2450

Table 2. Thermal and mechanical properties of tested semi-crystalline thermoplastics (Quadrant EPP Belgium).

Applied materials	Ertalyte® PET-P	TIVAR® 1000	SYMALIT® 1000	Techtron® 4208	ERTALON® 6 XAU
	polyethylene terephthalate	ultra-high molecular weight polyethylene	polyvinylidene fluoride	polyphenylene sulphide	polyamide 6
	PET	UHMWPE	PVDF	PPS	PA6
Density (g/cm ³)	1.39	0.93	1.78	1.35	1.15
Water absorption at saturation in air (23°C, 50% RH, %)	0.25	<0.10	0.05	0.03	2.20
Melting temperature (°C) DSC 10°C/min	245	135	175	280	215
Thermal conductivity at 23°C (W/mK)	0.29	0.4	0.19	0.30	0.29
Maximal service temperature in air (short periods, °C)	160	120	160	260	180
Maximal service temperature in air (20,000h, °C)	100	80	150	220	105
Ball indentation hardness (N/mm ²), dry material	170	33	110	205	165
Tensile strength (MPa)	90	---	60	102	86
Tensile modulus (MPa) *(23°C, 50% RH)	3500	750	2200	4000	*1700

2.2. Tribological characterisation

Tribological characterisation was performed with an in-house built semi-large-scale linear reciprocating sliding flat-on-flat tribotester. This set-up has been chosen because it allows for forces and contact surface dimensions close to real scale application. All tests were carried out in a conditioning chamber with ambient air at 23°C temperature and 50% relative humidity (RH). The central block of the tribo-tester with the positioning of thermocouples, the polymer samples and steel counterfaces can be seen in Figure 2. Both steel counterfaces are mounted to the central block, which slides in vertical direction. Both polymer samples are mounted in holders which are stiff in vertical direction, but compliant in horizontal direction in order to allow for wear (and displacement) of the specimens. The polymer sample size was 50x50x7 mm; the 100Cr6 steel counterface was 200x80x20 mm. Counterfaces were polished to surface roughness Ra = 0.2 µm. The friction/bulk temperature was measured by thermocouples located at 10 mm beneath the contact surface of the steel counterfaces.

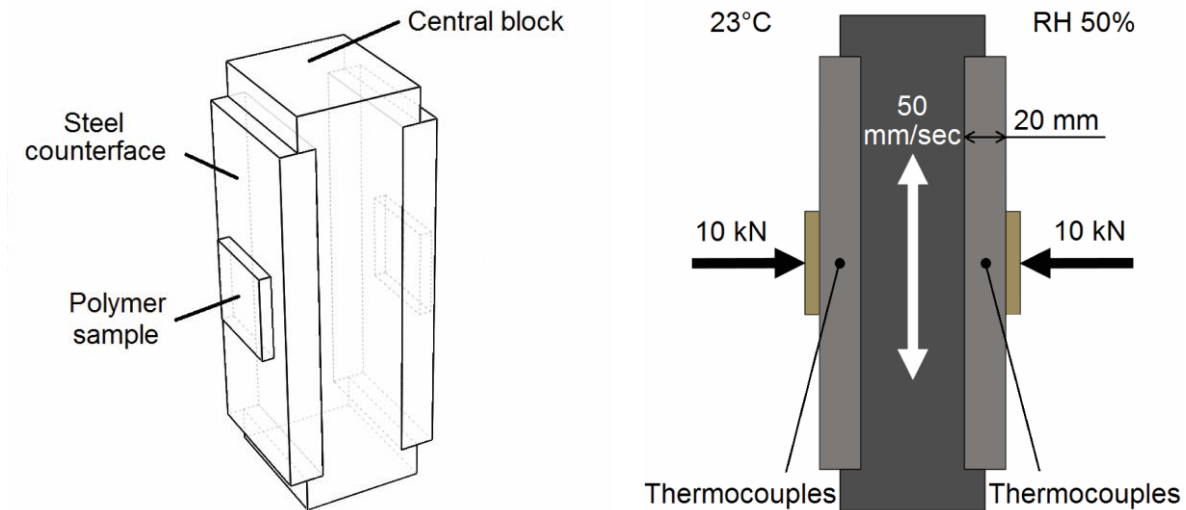


Figure 2. Schematic representation of linear reciprocating sliding flat-on-flat tribotester set up. All wear tests were performed in dry contact condition at 50 mm/s sliding speed and 10 kN normal force (corresponding to 4 MPa contact pressure). The total sliding distance was set up to 5000 cycles (1000 m). Measurements were recorded online with the use of NI 6036E DAQ (National instruments BNC 2100) in a LabVIEW platform. The coefficient of friction was evaluated with the following equation:

$$\mu = \frac{F_{Fr}}{n \cdot F_N} \quad (1)$$

μ is the coefficient of friction (-), F_{Fr} is the friction force (N), F_N is the normal force (N) and n is the number of samples/counterfaces, in this case $n = 2$. Figure 3 shows a typical friction curve of one test cycle. At the start of each stroke the coefficient of friction linearly increases what can be attributed to elastic deformation of the sample. Then the coefficient of friction reaches a maximum, the static coefficient of friction. The dynamic coefficient of friction is the average value of the red marked interval at the middle part of the stroke length.

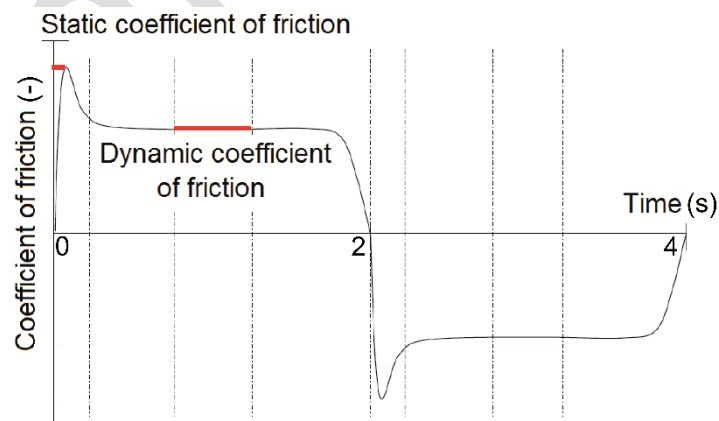


Figure 3. Friction curve during one test cycle

The specific wear rate of polymer samples was calculated with the following equation:

$$k = \frac{\Delta m}{\rho \cdot d} \quad (2)$$

k is the wear rate (m^3/mm), Δm is the measured mass loss (kg), ρ is the density (kg/m^3) and d is the sliding distance (mm).

Independent tests were performed at least three times under identical test conditions to study the uncertainty from the tribotester where a deviation of 10% in coefficient of friction and 20% in wear rate was observed. Prior to mass measurement (before as well as after wear testing) the polymer specimens were conditioned in an oven in order to exclude the influence of moisture absorption on mass measurements. The applied conditioning parameters were set at 70°C, as it is far enough from the melting range of all tested polymers and to 20 hours which is a sufficient interval to provide the same moisture condition before and after wear.

2.3. Material characterisation

The crystallinity, the melting temperature and the surface normal spring stiffness were determined because they can be brought into relation with to the wear performance and transfer layer formation during friction testing.

The degree of crystallinity of semi-crystalline thermoplastics was measured with Differential Scanning Calorimetry (DSC) and X-ray diffraction (XRD) while the melting temperature range was determined with DSC. The surface normal spring stiffness was measured by instrumented micro-indentation tests. DSC measurements were carried out with a TA Instruments Q2000 device. The samples were placed in Tzero hermetic aluminium pans and tested in a sequence of heat/cool/heat cycles, from 0°C to 300°C in the first heating cycle, from 300°C to -70°C in the first cooling cycle and from -70°C to 300°C in the second heating cycle. Both heating and cooling rate were 5°C/min. The samples were tested in 50 ml/min nitrogen purge flow. Degree of crystallinity was evaluated from the first DSC heating curve (Figure 4) with the following equation:

$$x\% = \frac{\Delta H_m}{\Delta H_{m100\%}} \cdot 100 \quad (3)$$

$x\%$ is the degree of crystallinity (%), ΔH_m is the integrated area of the melting peak (enthalpy of fusion) in first heating cycle (J/g), $\Delta H_{m100\%}$ is the enthalpy of fusion for 100% crystalline polymers (J/g).

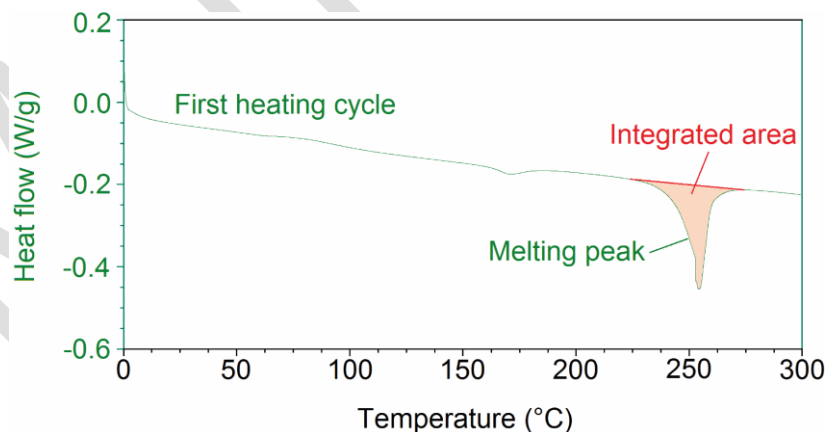


Figure 4. DSC curve of a semi-crystalline material (PET), first heating cycle, 5°C/min heating rate, 0-300°C temperature range.

XRD tests were carried out with a PANalytical X'Pert Pro MPD Diffractometer system equipped with an X'Celerator detector and Cu anode material. The instrumented micro-indentation tests were carried out at room temperature with a Zwick Z005 computer controlled tensile tester equipped with a 20 N capacity load cell. The pin used for the indentation was identical to the geometry defined for Shore D hardness measurement in ISO 868. The test was performed at 2 mm/min crosshead speed and a maximum load up to 10 N. The average and standard

deviation values were calculated from five measurements. The spring stiffness values were evaluated from the linear region of the recorded force – indentation depth graphs between 4 and 6 N to minimize the effect of the surface roughness and imperfections. The spring stiffness was calculated with the following equation:

$$k_s = \frac{F_2 - F_1}{x_2 - x_1} \quad (4)$$

k_s is the spring stiffness (N/m, given in kN/m), F_2 and F_1 are the measured forces which approached the value of 6 and 4 (N) respectively, x_2 and x_1 are the recorded indentation depths at 6 and 4 (N) respectively (m).

During friction testing the subsurface temperature (friction/bulk temperature) of the countersurface was measured by means of embedded thermocouples (see Figure 2).

3. Results and discussion

3.1. Friction and wear

The experimentally observed wear rate (m^3/m) and static and dynamic coefficients of friction (-) are presented in Table 3. PA6 was earlier investigated at large scale where the measured coefficient of friction values are in good agreement with the existing results [16]. Most of the nine polymers reached the proposed 1000 m sliding distance. Only PC and PEI failed during the initial phase, and did not reach the steady state friction. A clear relationship between the wear response and the corresponding wear mechanisms was observed. Wear mechanism can be grouped into three different categories: abrasive wear, combined adhesive-abrasive wear and adhesive wear. More detailed information about the background of this classification is available [8]. The macrographs and micrographs of some tested specimens are introduced in Figure 5 and 6. The occurrence of abrasive wear mechanism can be explained by the hard asperity of the steel counterfaces which were sliding on the surface of softer polymer samples [17]. Due to abrasive wear significant grooves appear on the worn surfaces of the tested polymers, which are parallel with the sliding direction [16, 17]. These deep grooves can be easily seen in Figure 5 (a) and Figure 6 (a) and (b). From Table 3 it can be seen that wear mechanisms of amorphous materials were abrasion and adhesion-abrasion. On the contrary the effect of pure abrasion was not found in the semi-crystalline grades. In case of semi-crystalline thermoplastics adhesion-abrasion and adhesion were observed as dominant wear mechanisms. Adhesive wear mechanism was observed for those thermoplastics which were able to form a transfer layer during sliding wear. Initially the transfer layer gets deposited in the roughness valley (from machine marks) of the metal counterface. Hence providing a smooth surface and avoiding severe indentation of hard asperity from the counter material on soft material (Figure 7). Thus the abrasion can be significantly reduced. Due to the formation of transfer layer, the initial metal-polymer sliding contact changes to partly or fully polymer-polymer sliding contact. The term of primary transfer layer is used when the transfer layer merely occupies the roughness valley of the counterface. In case of primary transfer layer, there is have no substantial deposition above the roughness peaks. The roughness profile acts as a mechanical obstruction to restrain the primary transfer layer. Abrasive wear mechanism does no longer occur, and the effect of adhesive wear mechanism is enhanced. In case of secondary transfer layer the formation is generated by accumulation of several layers. There is poor adhesion between the layers, which may cause the peeling of secondary transfer layer. The surface pattern of a secondary transfer layer appears as a lumpy uneven deposition covering the roughness peaks of the counterface material. Due to the secondary polymer transfer layer there is a circumstances, which causes additional adhesive wear.

Table 3. Static and dynamic coefficient of friction, wear rate, friction/bulk temperature, wear mechanisms and corresponding transfer layer characteristics.

Material	Static CoF (-)	Dynamic CoF (-)	Wear rate (m ³ /mm)	Friction/bulk temperature (°C)	Wear mechanism	Transfer layer characteristics
PC	0.50	0.49	2.36E-11	148	Abrasion	No transfer layer
PEI	0.54	0.48	1.79E-11	176		
PAI	0.62	0.54	1.60E-13	171		
PPSU	0.38	0.27	2.09E-13	158	Adhesion-abrasion	Secondary layer
PET	0.50	0.38	1.22E-13	195		
PPS	0.43	0.44	3.20E-13	227		
PA6	0.37	0.28	8.86E-15	169	Adhesion	Primary layer
PVDF	0.30	0.24	1.74E-14	155		
UHMWPE	0.27	0.21	2.53E-14	127		

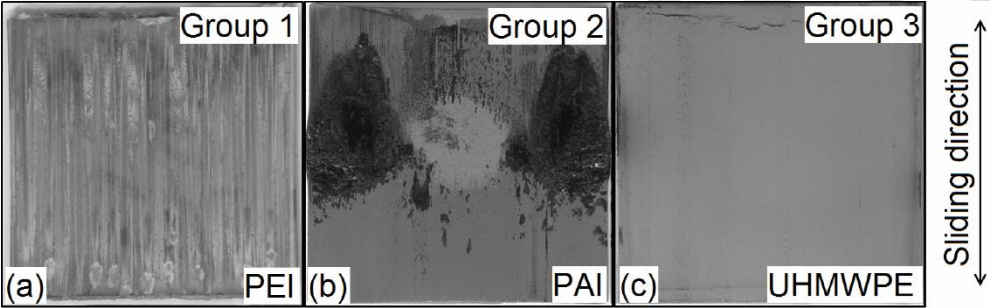


Figure 5. Photo-macrographs (50x50 mm) of PEI (a), PAI (b) and UHMWPE (c) after wear testing.

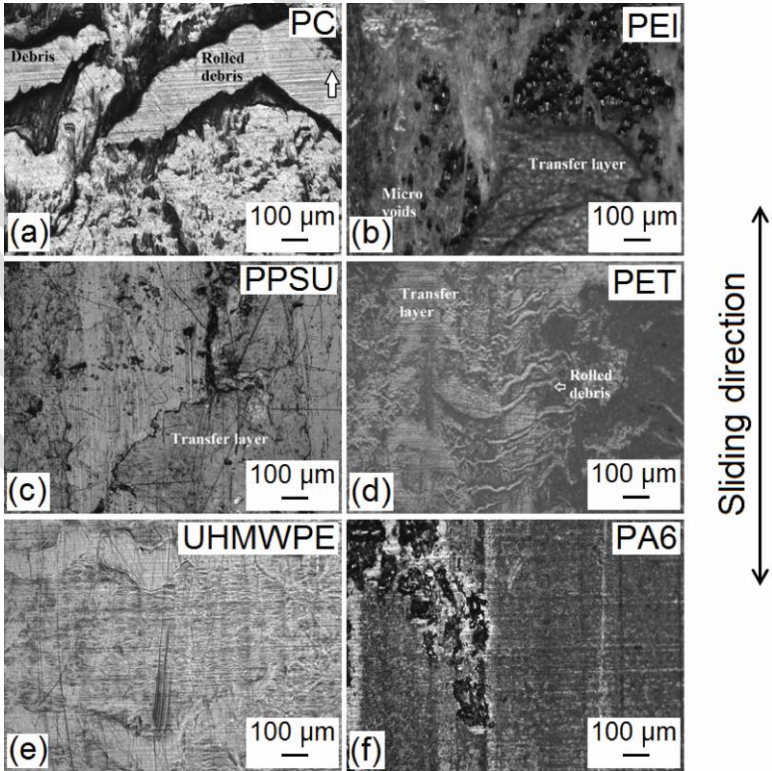


Figure 6. Micrographs of polymer samples, (a) and (b): abrasive wear; (c) and (d): combined adhesive-abrasive wear; (e) and (f): adhesive wear.

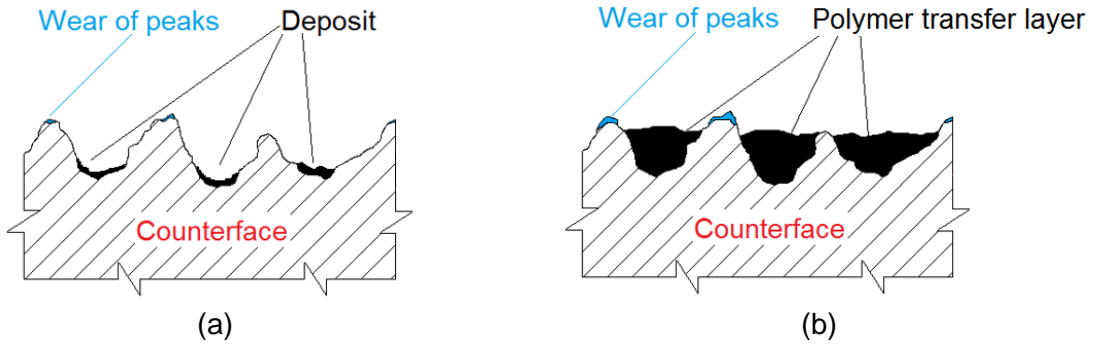


Figure 7. Transfer layer formation on steel counterface in sliding wear: high asperities of the steel (a), decreased surface roughness and asperities (b).

Transfer layer characteristics are highly dependent on the wear mechanism and vice versa. In case of adhesive-abrasive and adhesive wear mechanism the observed transfer layer characteristic is a secondary and a primary layer, respectively. These results also confirm that an adequate and uniform transfer layer acts as a protective agent and has a positive effect on the tribological performance of the materials. This positive effect results into low friction and low wear values, which is in agreement with the literature [15, 18, 19].

Abrasive wear mechanism (PC, PEI) shows two orders of magnitude higher wear rate than adhesive-abrasive (PAI, PPSU, PET, PPS), while the difference between adhesive-abrasive and adhesive wear mechanism (PA6, PVDF, UHMWPE) was about one order of magnitude in favour of the adhesive group. The abrasive wear mechanism includes ploughing and micro-cutting while the adhesive-abrasive wear mechanism contains mainly adhesion and micro-cutting. As it can be seen from Table 3 and Figure 8, the lowest coefficient of friction values corresponds to the adhesive wear mechanism. Figure 8 shows the specific wear rate as a function of the thermoplastic materials (amorphous samples = grey, semi-crystalline = green colour). The size of the markers symbolises the dynamic coefficient of friction. The measured low coefficient of friction of UHMWPE is also in line with the literature [20].

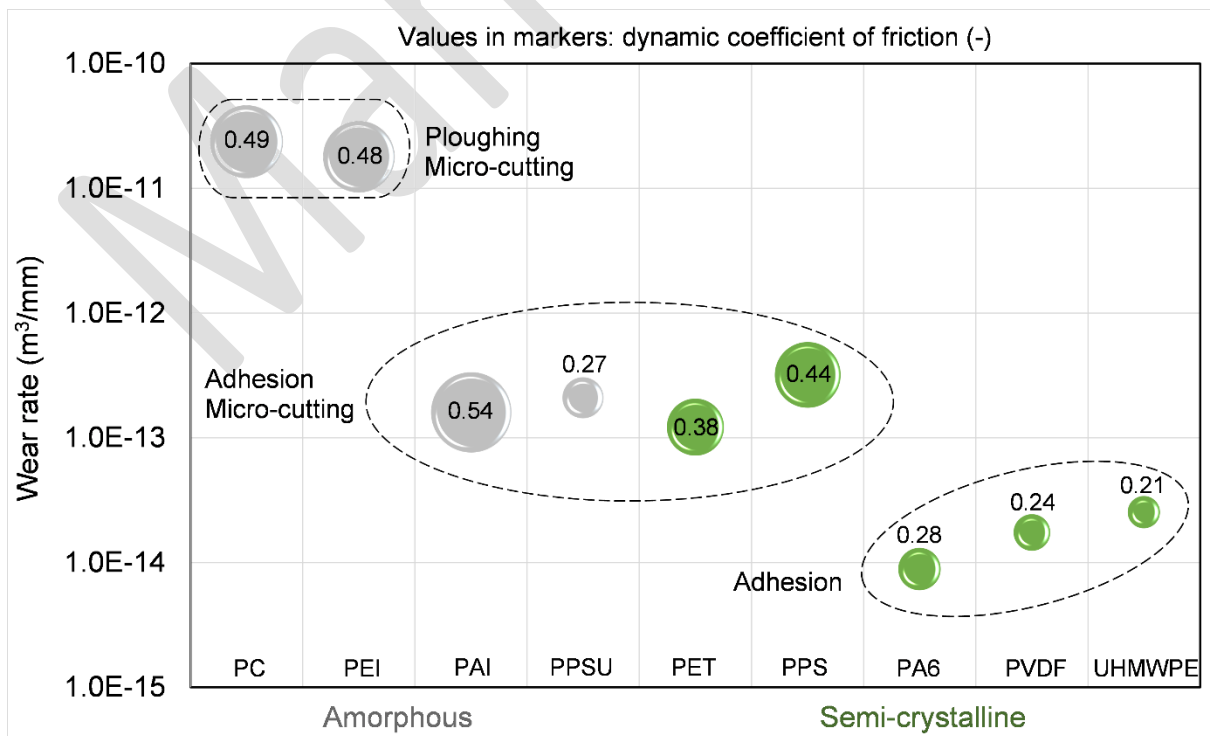


Figure 8. Wear rate and dynamic friction coefficient of thermoplastics.

3.2. Material characterisation

3.2.1. Mechanical properties

The tensile modulus values and the ball indentation hardness (from official datasheets of Quadrant EPP Belgium, Table 2) of the tested semi-crystalline thermoplastics are presented in Figure 9 (a) and (b). These materials according to their mechanical properties can be separated into two groups in the viewpoint of wear mechanism (adhesive-abrasive, adhesive). Materials with higher elasticity (Figure 9 (a)) and lower ball indentation hardness (Figure 9 (b)) as PA6, PVDF and UHMWPE are able to form a primary transfer layer. Due to their softer nature, mechanical bonding between the asperities of the steel counterface and the polymer transfer layer is higher. In this way the transferred materials which fills the valleys of the metal surface can serve as a protective agent. In case of PA6, tensile modulus value in equilibrium (23°C/50% RH) was chosen as it was also the case during wear testing. In Table 2 and Figure 9 (b) the referred ball indentation hardness value for PA6 was available in dry condition, which gives a higher value, than in equilibrium (23°C/50% RH).

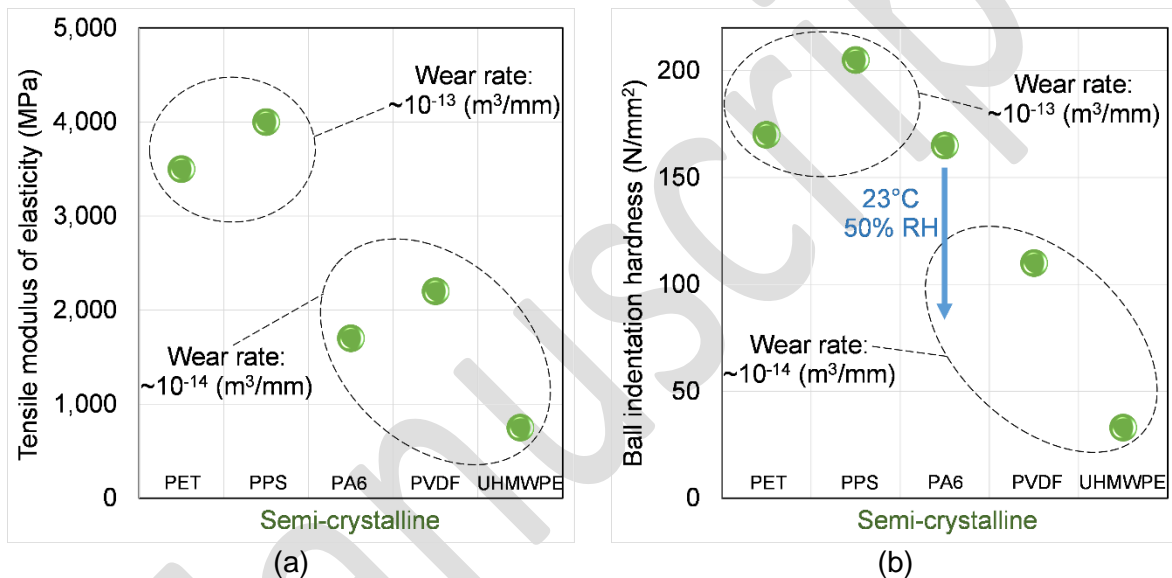


Figure 9. Tensile modulus of elasticity (a) and ball indentation hardness (b) of tested semi-crystalline samples (from datasheets of Quadrant EPP Belgium).

3.2.2. Degree of crystallinity measured by DSC and XRD method

The dissipated mechanical energy during the large scale wear test is converted into frictional heat, and the flash temperature of the contact surface can reach the melting or softening temperature of the applied polymers [21, 22]. Knowing that crystallinity is a critical factor and the crystallinity structure is influenced by the thermal profile of the contact surface during wear testing, the crystallinity was estimated before and after testing by DSC and XRD. It was evident from the results of DSC that the degree of crystallinity of worn semi-crystalline thermoplastics is relatively higher when compared to the untested specimen (Table 4, Figure 10). The most significant increase can be observed in case of PET and PPS samples, where the degree of crystallinity increased by 37.5 and 29.0% respectively. The increase in degree of crystallinity is reflected in an increase in hardness and reduction in plasticity. This is unbeneficial in the viewpoint of adequate transfer layer formation, in this way it has a negative influence to the wear rate. The valleys between the asperities of the metal counterface are not filled adequately and both adhesive and abrasive wear mechanism are more pronounced.

PPS debris did not show any crystallinity, the crystalline structure was destroyed, which is in agreement with the results of Chen et al [15]. A possible reason for the crystalline structure being destroyed is that a thin layer of the contact surface surpassed the melting temperature range of PPS, and the formed melt debris moved away from the sliding surface immediately. This resulted a high cooling rate for the investigated debris, restricting the formation of crystalline structure. The crystallinity of PET debris was not destroyed, their degree of crystallinity was similar to the worn surface of the sample.

Table 4. Degree of crystallinity of tested semi-crystalline materials before and after wear (measured by DSC).

Materials	Degree of crystallinity (%) Before wear	Degree of crystallinity (%) After wear	Difference (%)
PET	21.7	29.8	37.5
PPS	33.4	43.1	29.0
PA6	26.8	28.1	5.0
PVDF	39.9	46.4	16.4
UHMWPE	39.7	44.9	13.2
PET-debris	21.7	30.7	41.6
PPS-debris	33.4	0	---

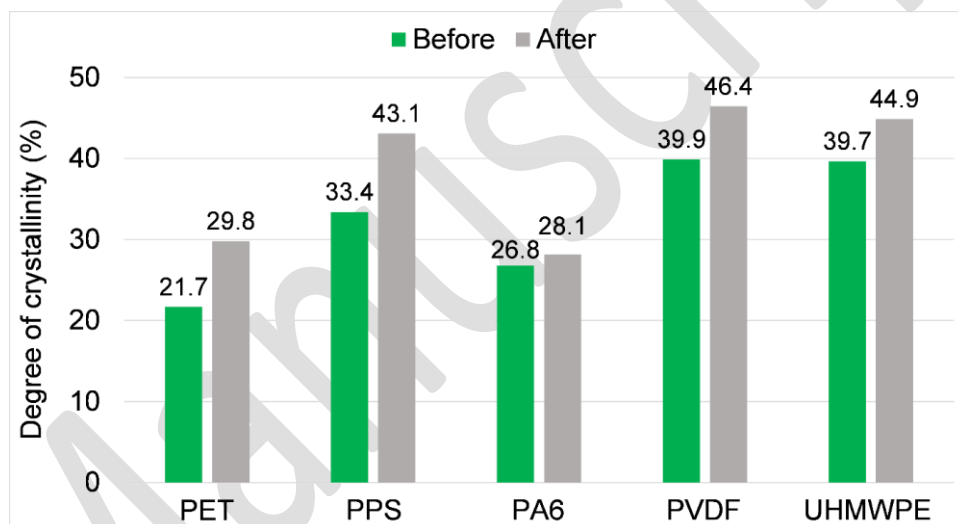


Figure 10. Degree of crystallinity of tested semi-crystalline materials before and after wear testing (measured by DSC).

The increasing of degree of crystallinity in semi-crystalline thermoplastics during wear test was also evidenced by XRD (X-ray diffraction) tests (Figure 11). It can be seen from Figure 11 (a) and (b) that the most significant changes are observed for PET and PPS. In PPS the intensity of the peaks before and after wear were respectively 2448 and 6278 (counts) which show a high increase in degree of crystallinity, confirming the results of DSC. The half-width of the peaks corresponding to the crystalline regions has also narrowed in case of both PET and PPS which indicates the increase in the crystallite sizes. This shows that not only the crystalline content has increased but also the crystalline regions became larger and more perfectly aligned, which leads to a significant improvement in hardness, modulus and strength of the worn top layer. In PET the height of all three peaks increased. In PA6, PVDF and UHMWPE a limited increase of after wear peaks can be observed (Figure 11 (c), (d) and (e)). The first peaks of PA6 and UHMWPE had different behaviour; the after wear peaks are slightly smaller than before wear. These reductions in first peaks are less significant than the increasing of the

second peaks. In these three polymer samples a limited degree of crystallinity increasing is also confirmed by XRD measurements.

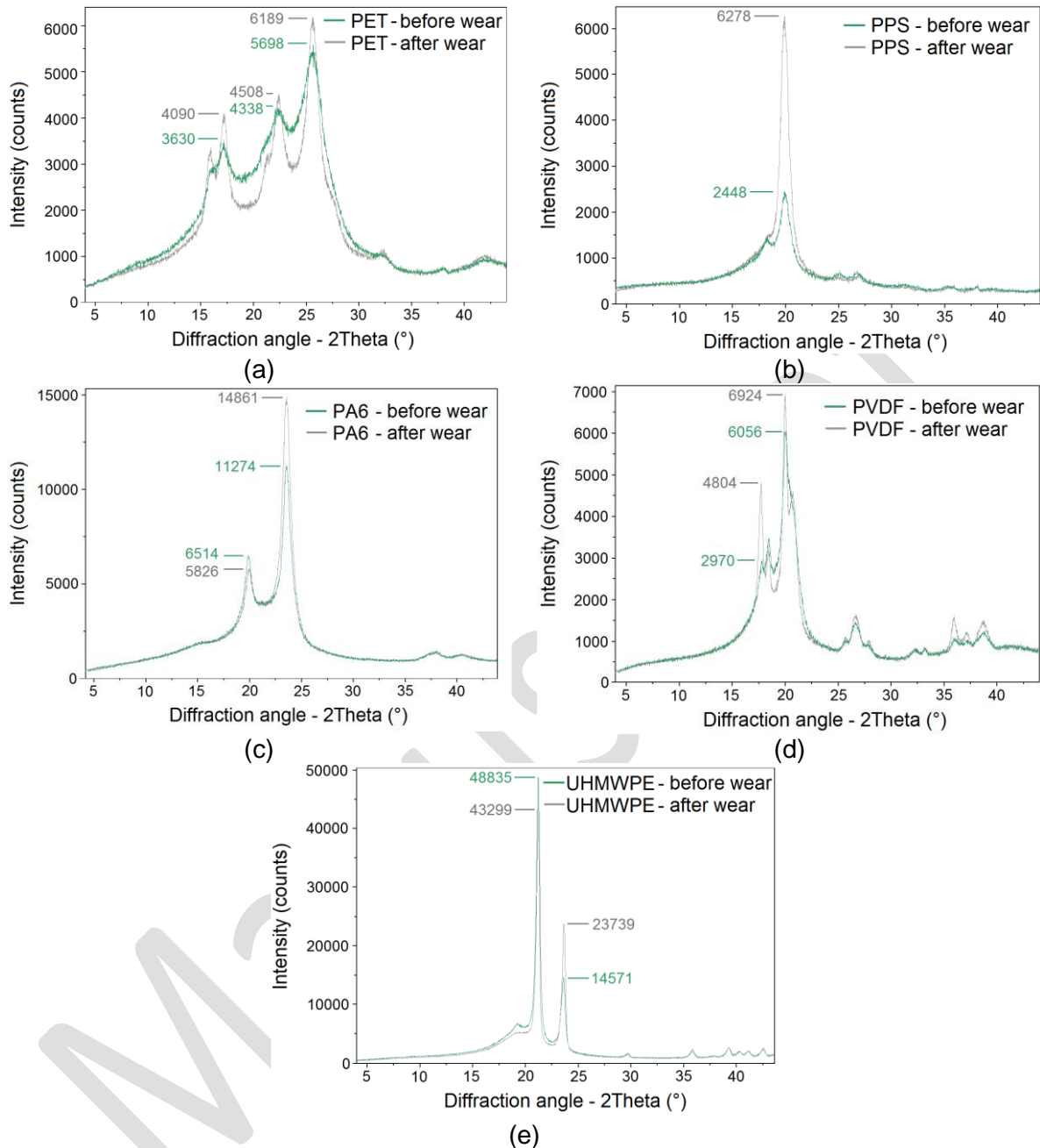


Figure 11. XRD curves of PET (a), PPS (b), PA6 (c), PVDF (d) and UHMWPE (e).

3.2.3. Relation of friction/bulk temperature to melting temperature

To assess the melting temperature range of the tested polymers, the melting curves of DSC tests were analysed. Table 5 and Figure 12-13 introduce the melting temperature and friction/bulk temperature of semi-crystalline thermoplastics. The friction/bulk temperature was measured in the steel counterfaces by thermocouples (Figure 2). The measured melting temperatures were in agreement with the data sheets of Quadrant EPP Belgium (Table 2). Significant differences between the melting temperature of worn and unworn thermoplastics was not observed (differences between 0 and 3°C). In amorphous thermoplastics a proper melting range cannot be easily defined with DSC. From DSC curves (Figure 13 (a) and (b)) it can be seen that the friction/bulk temperature approached the melting region in PA6 and

reached the melting region in PVDF and UHMWPE. The differences between the measured friction/bulk temperature and the melting temperature (DSC, 5°C/min) in PVDF and UHMWPE are 18°C and 7°C respectively. In PA6 the difference is 49°C but from the DSC curves (Figure 13 (b)) it can be seen that its friction/bulk temperature was close to the melting region. PET and PPS had respectively 59°C and 53°C lower friction/bulk temperature compared to their melting points (Figure 13 (a)). This can indicate that during the wear testing of PA6, PVDF and UHMWPE samples the melting temperature was reached at a larger depth of the top layer, providing a more significant self-lubrication. This also explains why PA6, PVDF and UHMWPE had adhesive wear mechanism with primary transfer layer formation. These three materials have lower hardness and lower stiffness, and additionally due to the molten thin top layer the transfer layer formation was further supported. The crystallinity increase was lower after the wear test for PA6, PVDF and UHMWPE samples compared to PET and PPS (Table 4, Figure 10). This can be attributed to two counteracting effects which would have caused this phenomenon: the first effect is the crystallinity increasing effect at elevated temperature, which was present in case of all of the semi-crystalline samples above the glass transition temperature (T_g), where the presence of segment movements (macro Brownian thermal motion) makes the refinement of molecular chain alignment possible. The second effect hinders the crystallinity and is caused by the melting process. Previously aligned molecular chains can move almost freely, and "resetting" of the crystallinity is observed near the melting temperature (T_m) in case of PA6, PVDF and UHMWPE.

Table 5. Measured melting temperature and friction/bulk temperature of tested semi-crystalline samples.

<i>Materials</i>	Melting temp (°C)	Friction/bulk temperature (°C)
	Before wear	(During wear testing)
PET	254	195
PPS	280	227
PA6	218	169
PVDF	173	155
UHMWPE	134	127

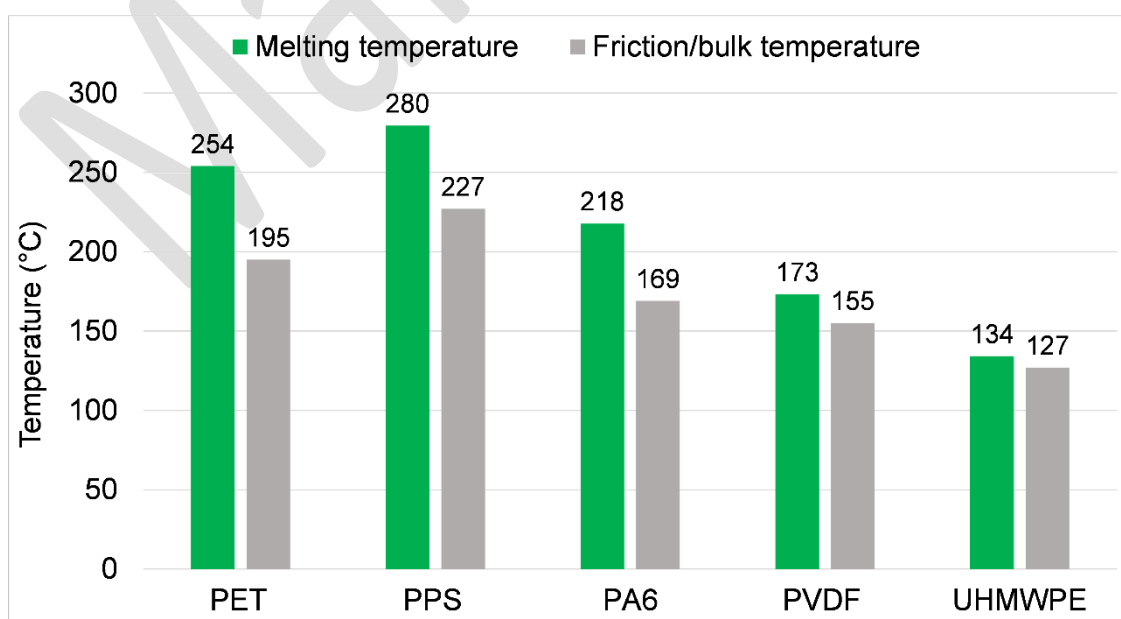


Figure 12. Melting temperature and friction/bulk temperature of tested semi-crystalline samples.

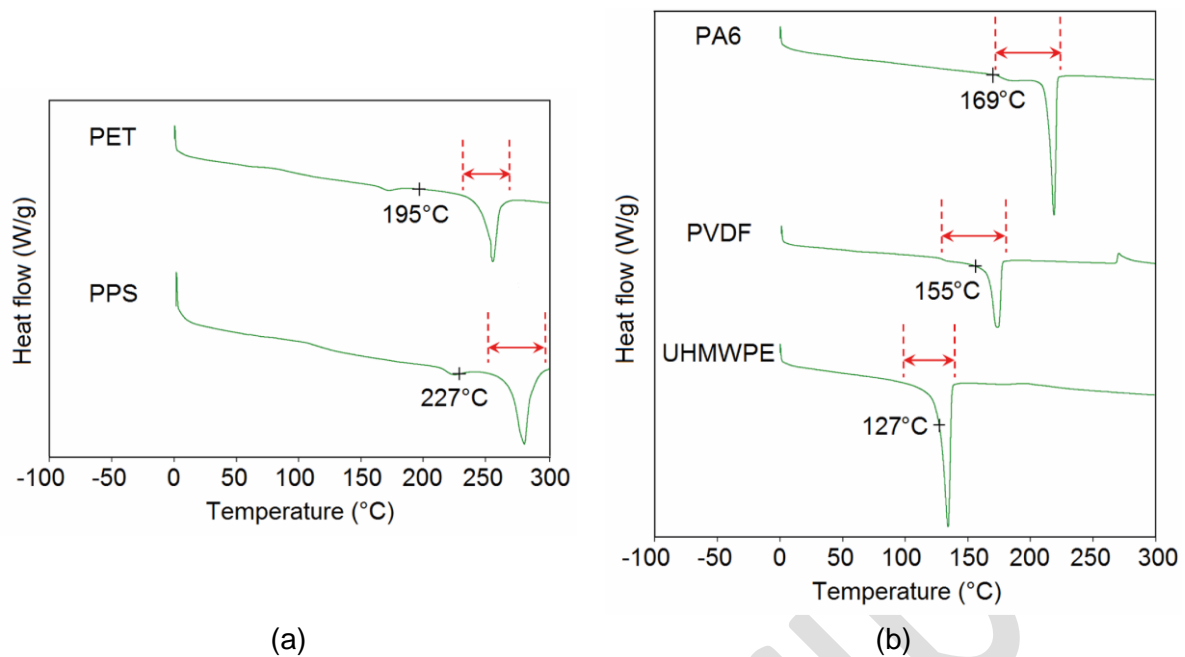


Figure 13. DSC curves of investigated semi-crystalline materials, first heating cycle, 5°C/min heating rate, 0-300°C temperature range. Friction/bulk temperature during wear test indicated by black cross, melting range is inside the red marked area. Adhesive-abrasive group is represented by (a), while adhesive group is represented by (b).

3.2.4. Micro-indentation test

Micro-indentation tests (Table 6, Figure 14) were selected to provide information about the surface hardness of the tested polymer samples. In case of the worn samples the conventional hardness measurement methods, for example Shore hardness measurement, had a too high indentation depth compared to the thickness of the heat affected region. In case of the instrumented indentation tests a maximum of 0.44 mm indentation depth was measured completely in the centre of the tested polymer sample where the heat affected zone is the most significant. The evaluated spring stiffness values were calculated between 4 and 6 N force. The differences in spring stiffness between the worn and unworn surfaces of amorphous samples were in the interval of the standard deviation. The results of semi-crystalline thermoplastics correlated well with the DSC and XRD tests. The spring stiffness, which corresponds to the microscale surface modulus of the material, increased after wear in PET, PPS, PA6 and PVDF. The degree of crystallinity is increased during wear test in these samples, and due to the modified morphology the spring stiffness is higher for all four samples. It is in agreement with literature that the increasing of degree of crystallinity results in an increased hardness [12]. It is important here, that all samples were measured in condition of (23°C, 50% RH), like the environment of the wear test. Due to water absorption the hardness/spring stiffness of PA6 is lower than the values mentioned in the datasheets of Quadrant, which have been obtained in dry conditions. All other samples have similar spring stiffness trend compared to the ball indentation hardness values provided by Quadrant (Table 1 and 2).

Table 6. Spring stiffness of tested thermoplastics before and after wear.

Spring stiffness kN/m	4-6 N		4-6 N	
	Before wear		After wear	
	Average	Deviation	Average	Deviation
PC	45.98	0.17	45.81	0.79
PEI	48.56	0.96	47.70	1.00
PAI	50.35	1.47	51.41	1.36
PPSU	42.16	0.58	40.80	0.46
PET	45.57	1.25	50.54	1.91
PPS	46.40	2.41	51.13	0.55
PA6	34.28	0.99	41.57	1.11
PVDF	35.77	0.97	40.87	0.35
UHMWPE	23.23	1.05	22.93	0.94

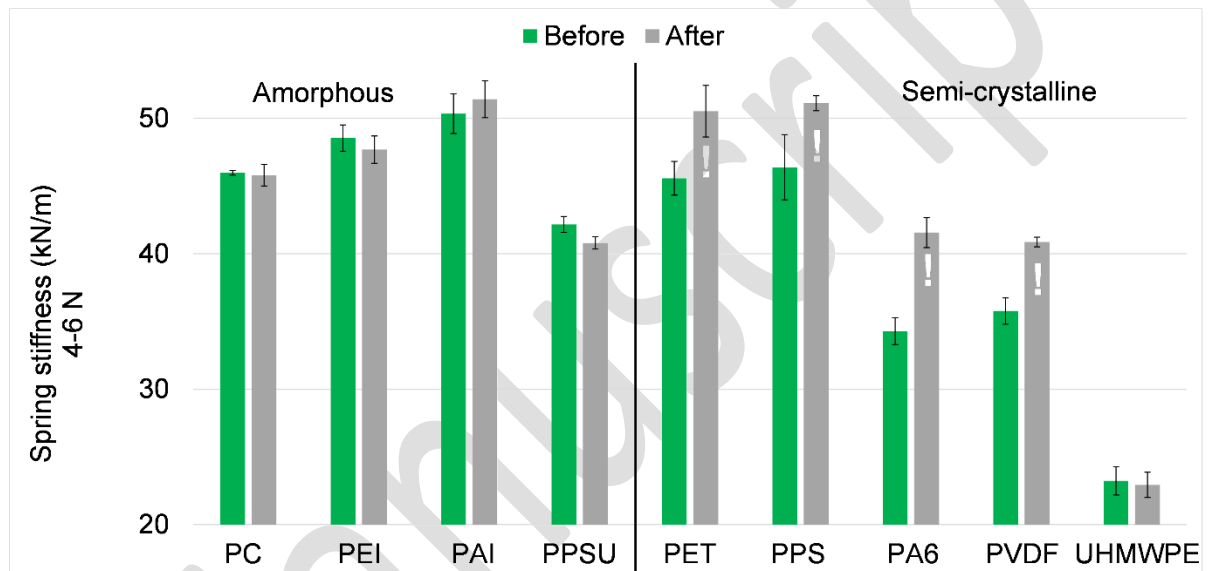


Figure 14. Spring stiffness of tested thermoplastics before and after wear.

4. Conclusions

In the present research we investigated four amorphous and five semi-crystalline thermoplastics.

- 1 The wear mechanism of these thermoplastics was grouped into three different categories as abrasive wear, combined adhesive-abrasive wear and adhesive wear. In case of amorphous thermoplastics abrasive (PC, PEI) and adhesive-abrasive (PAI, PPSU) wear mechanism was detected, while semi-crystalline thermoplastics showed adhesive-abrasive (PET, PPS) and adhesive (PA6, PVDF, UHMWPE) wear mechanism.
- 2 Semi-crystalline thermoplastics with adhesive wear mechanism reached the lowest coefficient of friction and wear rate (PA6, PVDF and UHMWPE).
- 3 Focusing to semi-crystalline thermoplastics we have defined and evaluated three key parameters directly connected to wear performance and the integrity of the transfer layer: crystallinity, the relation of friction/bulk temperature to melting temperature and the surface hardness.
- 4 The difference between the friction/bulk temperature and the melting temperature of semi-crystalline polymers plays a key role in their wear behaviour. Above T_g the crystallinity increases because of the presence of the segment movements of the polymer chains, causing an increase in surface hardness and stiffness, which results in an increased adhesive-abrasive wear mechanism. This was demonstrated in case of PET and PPS samples. In case of PA6, UHMWPE and PVDF the surface temperature approached or reached the melting temperature of the polymers at a larger depth, so this effect was countered by the melting of the surface layer, which caused lower surface modulus and adhesion as the resulting main wear mechanism.
- 5 The instrumented indentation tests also confirm in an indirect way the crystallinity increase in PET, PPS, PA6 and PVDF. As a result of the increase in degree of crystallinity and the originally high hardness values of PET and PPS, these materials show pronounced adhesive-abrasive wear mechanism with consequently a lower wear resistance compared to the other three semi-crystalline thermoplastics.

5. Acknowledgement

This investigation was supported and funded by Fonds Wetenschappelijk Onderzoek – Vlaanderen (FWO) 12S1918N. This research was performed under a cooperative effort between Ghent University (Belgium) and Budapest University of Technology and Economics (Hungary). Laboratory Soete would like to thank Hendrik Vandenbruaene of Quadrant EPP Belgium N. V. for the material support. The authors acknowledge the efforts of Professor József Karger-Kocsis from Budapest University of Technology and Economics and Dieter Fauconnier from Ghent University.

6. References

- [1] J.R. Fried, Polymer Science and Technology, third ed., Prentice Hall, 2014.
- [2] T.A. Osswald, G. Menges, Materials Science of Polymers for Engineers, third ed., Hanser, Munich, 2012.
- [3] L.H. Sperling, Introduction to Physical Polymer Science, fourth ed., John Wiley & Sons, Hoboken, New Jersey, 2006.

- [4] B.H. Stuart, Review Polymer crystallinity studied using Raman spectroscopy, *Vib. Spectrosc.* 10 (1996) 79-87.
- [5] D.G.M. Wright, R. Dunk, D. Bouvart, M. Autran, The effect of crystallinity on the properties of injection moulded polypropylene and polyacetal, *Polym. J.* 29 (1988) 793-796.
- [6] K.S.K. Karuppiyah, A.L. Bruck, S. Sundararajan, J. Wang, Z. Lin, Z.H. Xu, X. Li, Friction and wear behavior of ultra-high molecular weight polyethylene as a function of polymer crystallinity, *Acta Biomater.* 4 (2008) 1401-1410.
- [7] M. Conte, B. Pinedo, A. Igartua, Role of crystallinity on wear behavior of PTFE composites, *Wear* 307 (2013) 81–86.
- [8] J. Sukumaran, J. De Pauw, P.D. Neis, L.F. Tóth, P. De Baets, Revisiting polymer tribology for heavy duty application, *Wear* 376-377 (2017) 1321–1332.
- [9] P. Bhimaraj, D. Burris, W.G. Sawyer, C.G. Toney, R.W. Siegel, L.S. Schadler, Tribological investigation of the effects of particle size, loading and crystallinity on poly(ethylene) terephthalate nanocomposites, *Wear* 264 (2008) 632–637.
- [10] P. Bhimaraj, D.L. Burris, J. Action, W.G. Sawyer, C.G. Toney, R.W. Siegel, L.S. Schadler, Effect of matrix morphology on the wear and friction behavior of alumina nanoparticle/poly(ethylene) terephthalate composites, *Wear* 258 (2005) 1437-1443.
- [11] Y. Yamada, K. Tanaka, Effect of the degree of crystallinity on the friction and wear of poly(ethylene terephthalate) under water lubrication, *Wear* 111 (1986) 63-72.
- [12] K. Balani, V. Verma, A. Agarwal, R. Narayan, *Biosurfaces: A Materials Science and Engineering Perspective*, first ed., The American Ceramic Society, John Wiley & Sons, 2015.
- [13] P.H. Kang, Y.C. Nho, The effect of gamma-irradiation on ultra-high molecular weight polyethylene recrystallized under different cooling conditions, *Radiat. Phys. Chem.* 60 (2001) 79-87.
- [14] H.C.Y. Cartledge, C. Baillie, Y.W. Mai, Friction and wear mechanisms of a thermoplastic composite GF/PA6 subjected to different thermal histories, *Wear* 194 (1996) 178-184.
- [15] Z. Chen, T. Li, Y. Yang, X. Liu, R. Lv, Mechanical and tribological properties of PA/PPS blends, *Wear* 257 (2004) 696-707.
- [16] P. Samyn, P. De Baets, G. Schoukens, I. Van Driessche, Friction, wear and transfer of pure and internally lubricated cast polyamides at various testing scales, *Wear* 262 (2007) 1433–1449.
- [17] S. Soleimani, J. Sukumaran, A. Kumcu, P. De Baets, W. Philips, Quantifying abrasion and micro-pits in polymer wear using image processing techniques, *Wear* 319 (2014) 123–137.
- [18] E. Padenko, L.J. van Rooyen, B. Wetzel, J. Karger-Kocsis, “Ultralow” sliding wear polytetrafluoro ethylene nanocomposites with functionalized graphene, *J. Reinf. Plast. Compos.* 35 (2016) 892–901.
- [19] A.C. Greco, R. Erck, O. Ajayi, G. Fenske, Effect of reinforcement morphology on high-speed sliding friction and wear of PEEK polymers, *Wear* 271 (2011) 2222– 2229.
- [20] Y. Wang, Z. Yin, H. Li, G. Gao, X. Zhang, Friction and wear characteristics of ultrahigh molecular weight polyethylene (UHMWPE) composites containing glass fibers and carbon fibers under dry and water-lubricated conditions, *Wear* 380-381 (2017) 42–51.
- [21] M.Q. Zhang, L. Song, H.M. Zeng, K. Friedrich, J. Karger-Kocsis, Frictional surface temperature determination of high-temperature-resistant semicrystalline polymers by using their double melting features, *J. Appl. Polym. Sci.* 63 (1997) 589-593.

- [22] B. Bhushan, Modern Tribology Handbook Volume One, in: F.E. Kennedy, Frictional Heating and Contact Temperatures, CRC Press, 2001, pp. 235-272.

Manuscript